Soft Matter

PAPER

View Article Online
View Journal | View Issue

Cite this: *Soft Matter*, 2014, **10**, 2320

Direct evidence of gel–sol transition in cyclodextrin-based hydrogels as revealed by FTIR-ATR spectroscopy

Vincenza Crupi,[a] Domenico Majolino,[a] Andrea Mele,*[bc] Lucio Melone,[b] Carlo Punta,[bd] Barbara Rossi,*[ef] Fabio Toraldo,[b] Francesco Trotta[g] and Valentina Venuti*[a]

Received 5th September 2013
Accepted 3rd January 2014

DOI: 10.1039/c3sm52354c

www.rsc.org/softmatter

The phase transition from gel to liquid suspension in cyclodextrin (CD)-based hydrogels is in depth monitored by using Fourier transform infrared spectroscopy in attenuated total reflectance geometry. Cyclodextrin nanosponges (CDNS) synthesized by polymerization of CD with the cross-linking agent ethylenediaminetetraacetic dianhydride at different cross-linking agent/CD molar ratios have been left to evolve from gel phase into liquid suspension upon gradual increase of the hydration level. Measurements of the changes occurring in the vibrational dynamics of the system during this transition provide direct evidence of the gel–sol progress of the CNDS hydrogel, by accounting for the connectivity pattern of water molecules concurring to the gelation process. The experimental results clearly indicate that the increase of the hydration level is accompanied by the corresponding increase of the population of H_2O molecules engaged in high-connectivity hydrogen-bond networks. The water tetrahedral arrangement is thus dominant above a characteristic cross-over hydration level, experimentally determined for all the investigated samples. The observation of this characteristic cross-over point for the CDNS hydrogel and its correlation with other parameters of the system (*e.g.* the absorption ability of CDNS and elasticity of the polymer matrix) is, once again, modulated by the cross-linking agent/CD molar ratio. The latter seems indeed to play a key role in defining the nano- and microscopic properties of nanosponge hydrogels.

Introduction

The relevance of physical and chemical interactions in nano-structured self-assembled systems has recently emerged in the framework of the rational design of new soft materials.[1] Three-dimensional networks of cross-linked polymers are considered a very versatile class of components of a bottom-up approach toward self-assembled materials with tailored properties at different length-scales.[2] The possibility of tuning the chemical–physical interactions occurring among the different components of these assemblies makes it possible to control the structural properties of the system at the nano- and microscales and obtain particular phases of the matter, *i.e.* liquid or gel states. All these materials rouse tremendous interest in fast-growing fields of technology, like drug delivery, tissue engineering and regenerative medicine.[3–5]

Cyclodextrin nanosponges (CDNS) are a highly versatile class of cross-linked polymers[6–8] able to generate hydrogels with intriguing properties. CDNS are prepared by polycondensation between cyclodextrins (CD) and suitable cross-linking agents, such as carbonyldiimidazole (CDI),[9–11] pyromellitic anhydride (PMA)[12–15] or activated derivatives of ethylenediaminetetraacetic acid (EDTA).[16] The reaction leads to the formation of a three-dimensional network of CD units, interestingly showing both hydrophilic and hydrophobic nano-sized cavities where different types of organic and inorganic species can be encapsulated, transported and selectively released.[6–8]

Thanks to this unique structure, cyclodextrin nanosponges can form complexes with both lipophilic and hydrophilic molecules, thus allowing us to extend the possible application of these systems with respect to conventional hydrogels. These properties lead to significant applications in agriculture,[17] environmental control,[18,19] and cosmetic and pharmaceutical fields.[20–27]

More interestingly, cyclodextrin nanosponges are super-absorbents for water, *i.e.* they are efficient water nano-containers, showing marked swelling behaviour in the presence

[a]*Dipartimento di Fisica e di Scienze della Terra, Università di Messina, Viale Ferdinando Stagno D'Alcontres 31, 98166 Messina, Italy. E-mail: vvenuti@unime.it; Fax: +39 090395004; Tel: +39 0906765070*

[b]*Department of Chemistry, Materials and Chemical Engineering "G. Natta", Politecnico di Milano, Piazza L. Da Vinci 32, 20133, Milano, Italy. E-mail: andrea.mele@polimi.it; Fax: +39 0223993180; Tel: +39 0223993006*

[c]*CNR-Institute of Chemistry of Molecular Recognition, via L. Mancinelli 7, 20131 Milano, Italy*

[d]*INSTM Local Unit, Politecnico di Milano, Milano, Italy*

[e]*Dipartimento di Fisica, Università di Trento, via Sommarive 14, 38123 Povo, Trento, Italy. E-mail: rossi@science.unitn.it; Fax: +39 0461281690; Tel: +39 0461282940*

[f]*INSTM, Local Unit of Trento, Trento, Italy*

[g]*Dipartimento di Chimica, Università di Torino, Via Pietro Giuria, 10125 Torino, Italy*

of aqueous solutions.[12,14,15] The addition of water to the insoluble CDNS polymer matrices provides, in some cases, highly viscous, gel-like dispersion, similarly to hydrogels.[5,28,29] Recently, CDNS hydrogels have been used as a chiral reaction environment for photochemical asymmetric synthesis with noticeable capability of asymmetric induction.[30] Moreover, the diffusion properties of water molecules and solutes inside CDNS gels were investigated by using HR-MAS NMR spectroscopy.[12]

In the last few years we focused our research on the understanding of how the hydrogen-bond network and covalent cross-links determine the swelling and macroscopic properties of nanosponge hydrogels.

By the combined use of inelastic light scattering experiments, infrared spectroscopy and numerical computations, the structural and dynamic properties of dry polymers were explored at the molecular level, as a function of some parameters which can be varied during the synthesis of CDNS.[9–13,16] The results clearly evidenced that the cross-linking degree and the elastic properties of the polymer matrix can be successfully modulated by varying the chemical structure of the cross-linking agent and by acting on the relative amount of the cross-linker with respect to the monomer CD (*i.e.* n = cross-linking agent molar excess with respect to CD) during the synthesis procedure. Surprisingly, in all the systems a triggering of stiffness and connectivity was systematically observed in correspondence of a 6-fold excess of cross-linker with respect to CD: this finding gives evidence that at $n = 6$ a balance between two competing effects (reticulation and branching of CD units) is reached.[10,16]

On the other side, this puzzling scenario was further recently enriched by the accurate inspection of the effect of the confinement of H_2O and D_2O in the porous structure of nanosponges.[12,14,15] The entire amount of the experimental results suggests that the physical and covalent bonds within the CDNS hydrogels combine to determine the macroscopic properties of the gel phase, like the water holding capacity and the rigidity of the gel network, in a complex interplay over different length-scales.[15]

In this work, we extend our investigation on the effect of water confinement in the nano-sized cavities of CDNS, giving direct evidence of the phase transition process from gel to liquid phase[1,31,32] observed in these cyclodextrin-based hydrogels.

Ester-bridged CDNS based on pyromellitic anhydride have been recently shown to undergo a sol–gel phase transition upon gradual increase of the concentration of CDNS from 0.2 to 2000 mg mL^{-1} in water.[30] Transparent precipitates were formed at 1.0 mg mL^{-1} concentration of CDNS, whose particle size gradually increased by increasing CDNS contents. At higher contents, the solution became a gel-like diphasic system containing both liquid and gel phases or "flowing gel", and eventually gave a rigid gel at critical gelation ratios depending on the type of CDNS. The hydrogen-bond network of water molecules in the polymeric gel as well as the water–polymer interactions are expected to play a crucial role in the progressive sol-to-gel phase evolution.

In the present work nanosponge hydrogels obtained by polymerization of β-CD with an activated derivative of ethylenediaminetetraacetic acid (EDTA) at different CD/EDTA molar ratios have been left to evolve from gel into sol state upon gradual increase of the hydration level. At the same time, the changes observed in the vibrational spectral features assigned to the O–H stretching and HOH bending bands of water molecules progressively confined in the nano-pores of the polymer were monitored during the evolution of the system by using Fourier transform infrared spectroscopy in attenuated total reflectance geometry (FTIR-ATR).

A detailed evaluation of the observed modifications in the OH stretching profile was achieved by decomposition of the band into individual sub-components associated with different levels of water connectivity. The experimental findings are explained by accounting the fraction of water molecules involved and not involved in hydrogen-bond tetrahedral arrangements. As a main result, a cross-over hydration level from gel to liquid state was observed and correlated with the other parameters of the system (*i.e.* the absorption ability of CDNS and elasticity of the polymer matrix) surprisingly revealing, once again, the fundamental role played by the molar ratio n to define the nano- and microscopic properties of nanosponge hydrogels.

Materials and methods

A Chemicals

The nanosponges were obtained following a synthesis procedure previously reported.[6–8] In order to obtain β-CDEDTA1n nanosponges, anhydrous β-CD (1.135 g ÷ 1 mmol) was dissolved at room temperature in anhydrous DMSO (4 mL) containing 1 mL of anhydrous Et_3N. Then, the cross-linking agent ethylenediaminetetraacetic acid dianhydride was added at molecular ratios of 1 : n (with $n = 4$, 6, 8, and 10) under intense magnetic stirring. The polymerization was complete in few minutes obtaining a solid that was broken up with a spatula and washed with acetone in a Soxhlet apparatus for 24 h. The pale yellow solid was finally dried under vacuum.

The corresponding hydrogel of nanosponges was prepared by adding the dry samples of β-CDEDTA1n ($n = 4$, 6, 8, and 10) to a suitable amount of double-distilled water (Sigma) in order to obtain different levels of hydration h in the range 1.4–25.8. The hydration level h is defined as weight ratio H_2O/β-CDEDTA1n. Water containing traces of Rhodamine B dye (<0.1 mg L^{-1}) was uniquely employed to better visualize the phase evolution of specific samples in photographs.

All the gel samples were freshly prepared and used for FTIR-ATR measurements. All these measurements were conducted in the absence of Rhodamine B.

B FTIR-ATR measurements

FTIR-ATR measurements were performed by means of a BOMEM DA8 Fourier transform spectrometer, using a Globar source, a KBr beamsplitter, and a thermo-electrically cooled deuterated triglycine sulphate (DTGS) detector. Spectra were

collected at room temperature in the 400–4000 cm^{-1} wavenumber range. Samples were contained in a Golden Gate diamond ATR system, based on the attenuated total reflectance (ATR) technique.[33] Each spectrum was recorded in a dry atmosphere, in order to avoid dirty contributions, with a resolution of 4 cm^{-1}, and is an average of 100 repetitive scans, so guaranteeing a good signal-to-noise ratio and high reproducibility. No mathematical correction (*e.g.* smoothing) was done, and spectroscopic manipulation such as baseline adjustment and normalization was performed using the Spectracalc software package GRAMS (Galactic Industries, Salem, NH, USA). Band decomposition of the O–H stretching spectral range (2800–3800 cm^{-1}) was undertaken using the curve fitting routine provided in the PeakFit 4.0 software package, which enabled the type of fitting function to be selected. The strategy adopted was to use well-defined shape components of Voigt functions with all the parameters allowed to vary upon iteration. The statistical parameters were used as a guide to 'best fit' characterized by $r^2 \approx 0.9999$ for all the investigated systems.

Results and discussion

Fig. 1(a)–(j) show photographs of the phase evolution of a sample of the β-CDEDTA14 hydrogel observed as increasing the water content with respect to the amount of nanosponge. The initially rigid opaque gel (the sample does not flow if turned upside down, as evident from Fig. 1(a)), obtained at low hydration levels, progressively tends to flow with the increase of the water content up to a level at which it becomes a fluid suspension for high values of h (Fig. 1(j)). The characteristic hydration levels h of gelation, as probed by vibrational spectroscopy, depend on the type of nanosponge and they are generally in the range 2–20.

In Fig. 2(a) and (b), the FTIR-ATR spectra of β-CDEDTA14 and β-CDEDTA110 hydrogels at two different values of hydration $h = 2.7$ and $h = 16.4$ are reported, in the wavenumber region between 2800 and 3800 cm^{-1}, as example.

This specific spectral regime, where typically the O–H stretching band of H_2O molecules falls, is particularly informative of the three-dimensional interconnected network of hydrogen-bonds in which the molecules of water are involved.[34,35]

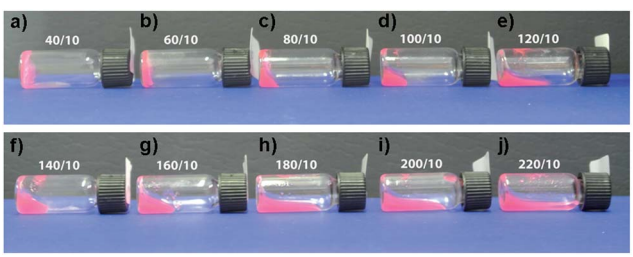

Fig. 1 (a–j) Photographs of samples of the β-CDEDTA14 hydrogel obtained as increasing the weight ratios H_2O/β-CDEDTA14. Note: a suitable dye (Rhodamine B) was added to the water solvent in order to better visualize the phase changes of the system. The hydration level h is reported above each vial.

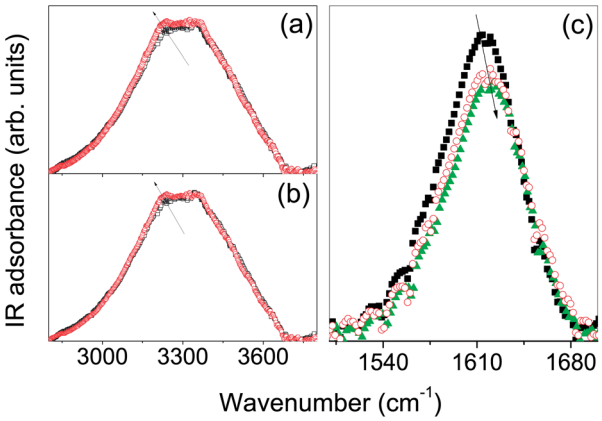

Fig. 2 Experimental FTIR-ATR spectra in the O–H stretching region for β-CDEDTA14 (a) and β-CDEDTA110 (b) hydrogels at $h = 2.7$ (black closed squares) and $h = 16.4$ (red open circles). (c) Experimental FTIR-ATR spectra in the HOH bending region for the β-CDEDTA18 hydrogel at $h = 2.7$ (black closed squares), $h = 11.8$ (red open circles) and $h = 20.2$ (green closed up triangles).

As is well known,[36–38] any spectral variation, in shape and/or centre-frequency, of the OH stretching profile can be related to the changes in the characteristic strength, distances and co-operativity of the hydrogen bond arrangement involving the water molecules which are attached or confined in the pores of the CDNS polymeric matrix.

The analysis of the spectra acquired at different h values points out remarkable changes in the OH stretching profile by varying the hydration level, as indicated by the arrows in Fig. 2(a) and (b). This experimental finding suggests a redistribution of water molecules among the different hydrogen bond sites as changing h. As a general trend, we observe that an increase of the hydration level corresponds to an enhancement of the low-frequency contribution of the OH stretching band, suggesting an increase of the co-operativity in the H-bond scheme.

These results appear consistent with what already observed in PMA-nanosponges[14] and can be explained by hypothesizing that by increasing the water content a first layer of H_2O molecules tends to saturate the active sites of the polymer surface, then rearranging in highly coordinated, bulk-like environments.

A further confirmation of this interpretation is provided by the behaviour observed for the HOH bending band of water molecules which appears as a relative intense and broad band centred at ~1615 cm^{-1} (Fig. 2(c)). This band, assigned to water molecules not involved in a symmetric tetrahedral network,[39,40] progressively shifts towards higher wavenumbers with increasing h values and, at the same time, decreases in intensity as shown in Fig. 2(c) for the β-CDEDTA18 hydrogel, as an example.

The quantitative analysis of the observed O–H profiles is then carried out by the curve fitting and deconvolution procedure already described in the literature.[41–44] Accordingly, the O–H stretching profile of water can be decomposed into four classes of O–H oscillators, corresponding to four transient

H-bonded and non-H-bonded structures (Fig. 3). In particular, the two sub-bands at the lowest wavenumber, namely ω_1 and ω_2, have been assigned to the symmetric and asymmetric O–H stretching mode of water molecules arranged in a tetrahedral network and exhibiting strong hydrogen bonding on both the hydrogen atoms. The spectral component ω_3 reflects the non-in-phase O–H stretching mode of tetrahedral arrangements commonly referred to as 'bifurcated H-bonds', originating distorted tetrahedral structures. Finally, the highest wavenumber sub-band ω_4 is representative of the O–H mode of water molecules whose H-bond network is, totally or at least partially, broken.

An example of best curve-fitting results is shown for β-CDEDTA16 and β-CDEDTA18 hydrogels at $h = 4.3$ and $h = 20.2$, respectively, in Fig. 3(a) and (b).

The presence, in the experimental spectra, of four sub-bands with the assigned centre-frequencies was suggested by the analysis of the second derivative profiles (not reported here) that showed four minima approximately corresponding to the maxima of each band component. This procedure allowed us to overcome, in a way, the well-known difficulties related to the possibility of uniquely fitting IR band profiles.[45,46] Finally, we remark that the protocol adopted here makes use of the minimum number of parameters, furnishing at the same time best-fits characterized by $r^2 \sim 0.9999$ for all the analysed samples.

Fig. 4(a)–(d) show, for all the investigated β-CDEDTA1n hydrogels, the evolution of the estimated percentage intensities I_i ($i = 1$, 2, 3, and 4) of the different spectral contribution

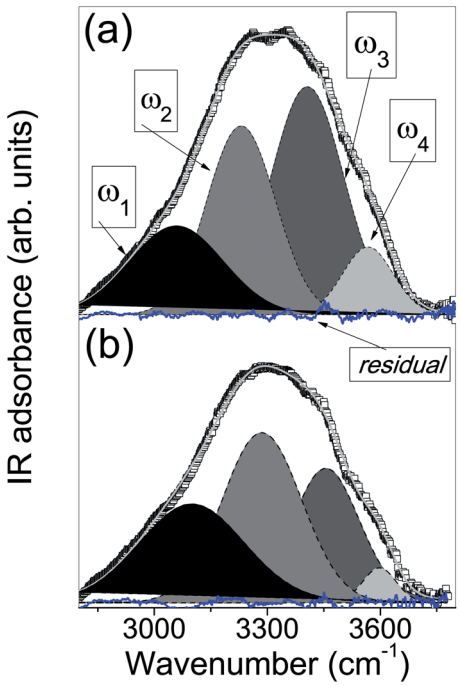

Fig. 3 Examples of fitting results of the O–H stretching profile for the β-CDEDTA16 hydrogel at $h = 4.3$ (a) and the β-CDEDTA18 hydrogel at $h = 20.2$ (b). The experimental data (empty squares) are reported together with the best-fit (grey line), the deconvolution components (indicated in the individual subpanels) and the residuals (blue lines).

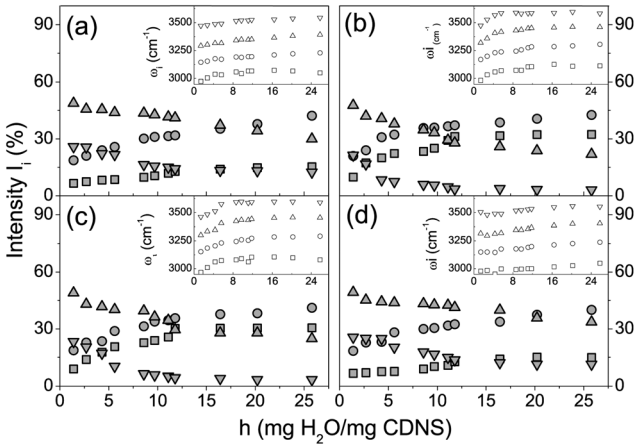

Fig. 4 Percentage intensities I_i of the different spectral contributions to the O–H stretching band as a function of the hydration level h for (a) β-CDEDTA14, (b) β-CDEDTA16, (c) β-CDEDTA18, and (d) β-CDEDTA110 hydrogels. I_1: closed squares, I_2: closed circles, I_3: closed up triangles, I_4: closed down triangles. For each plot, the inset reports the evolution of the corresponding peak wavenumbers: ω_1: open squares, ω_2: open circles, ω_3: open up triangles, and ω_4: open down triangles.

representative of the population of each class of OH oscillators as a function of the hydration h. The insets of each subpanel report also the behavior of the peak wavenumbers ω_i as a function of h. The center frequencies ω_i are related to the strength of the corresponding type of H-bonds.

From the inspection of Fig. 4, it clearly appears that an increase of the water content corresponds to an enhancement of the population of water molecules arranged in highly coordinated, hydrogen bonded networks (I_1 and I_2), *i.e.* bulk-like contribution. Correspondingly, a decrease of the population of water molecules involved in less cooperative structures which are typically associated with water molecules "perturbed" by the presence of solutes or attached to some interface (I_3 and I_4), is found with increasing h. Moreover, a characteristic saturation effect is observed at the high values of h for the populations I_1 and I_4.

For all the analysed samples, any single H-bond environment is slightly reinforced by increasing the hydration level, as indicated by the behaviour of the peak wavenumbers ω_i reported in the insets of Fig. 4.

These findings could be explained by invoking an increase in the pore size of nanosponges, as increasing h, up to a certain value of the hydration level beyond which the nano-cavities of CDNS are no longer able to enlarge, despite the fact that other water molecules are added. This interpretation is consistent also with small angle neutron scattering measurements recently performed on the CDNS hydrogel which will be reported elsewhere.

The conclusion that high values of h induce an enlargement of pore sizes of nanosponges can be further supported by previous Raman spectroscopy investigations, aimed at exploring the influence of nanoscopic confinement on the vibrational properties of liquid water confined in Gelsil glass

with pores of different dimensions.[47] In that case, a detailed evaluation of the observed changes in the O–H stretching profile gave evidence that the population associated with fully tetrahedrally hydrogen bonded water molecules is lower in the case of water confined in Gelsil 75 Å with respect to Gelsil 200 Å, allowing us to hypothesize that enlarging pore diameter produces on the connectivity pattern of water an effect similar to that obtained by lowering temperature.

In order to give a more synthetic view of the phenomena, we consider the intensities $(I_1 + I_2)$ and $(I_3 + I_4)$ which are representative of the population of the bulk-like (*i.e.* tetra-coordinated) and not bulk-like water molecules, respectively. The behaviour of these quantities is reported as a function of hydration h in Fig. 5(a)–(d) for all the analysed β-CDEDTA1*n* hydrogel. The experimental data were fitted by using a simple second-order polynomial function (dashed lines in Fig. 5) which well describes the evolution of the experimental points.

The curves reported in Fig. 5 clearly give evidence of the existence of a characteristic crossover point. Such point is indicative of the experimental conditions where the tetrahedral arrangements of the water molecules become favoured with respect to the structures having connectivity less than four (vertical lines in panels of Fig. 5). An estimation of the hydration level h_{cross} at the cross-over condition can be obtained directly from the curves of Fig. 5 for each of the investigated hydrogels. h_{cross} can be seen as a descriptor of the maximum hydration level above which the pores of the nanosponge are saturated. At higher water content, H_2O molecules tend to rearrange in more cooperative, bulk-like networks, due to the lack of available space inside the pores of the polymeric matrix. Correspondingly, for $h > h_{cross}$ the phase transition from a rigid gel-forming system to a fluid suspension is observed, as revealed in the photographs of Fig. 6.

In Fig. 7, the estimation of h_{cross} is reported as a function of the parameter n which represents the molar ratio between cross-linking agent EDTA and the monomer CD used in the synthesis of the nanosponge polymer matrix.

Two different regions corresponding to a phase of a rigid gel state and fluid suspension can be identified for $h < h_{cross}$ and $h > h_{cross}$, respectively, as evidenced in Fig. 7.

Interestingly, the plot shown in Fig. 7 points out an inversion point in correspondence of a 6-fold excess of cross-linker with respect to CD, closely recalling what has already been observed on different classes of nanosponges by low-frequency Raman, Brillouin and FTIR-ATR experiments, in dry and gel states. Considering the dry CDNS[9–13,16] the six-fold excess of the cross-linking agent with respect to CD corresponded to the maximum extent of bond connectivity and stiffness of the polymers. A further excess of the cross-linking agent was shown to provide branching of cyclodextrin units rather than a further increase of the polymerization. Upon hydration,[14,15] it was found that the molar ratio $n = 6$ corresponds also to the formation of the most strongly interconnected hydrogen-bonded network in the hydrogel.[15] On the other side, higher values of n were found to decrease the degree of the hydrogen bond network due to the destructuring effects associated with the increased steric hindrance of the polymeric network introduced by the excess of cross-linker.

The plot of Fig. 7 seems to indicate that the saturation of the confinement sites of water (*i.e.* the pores of the nanosponge) is reached, in the case of $n = 6$, at lower hydration levels with respect to the other nanosponges. This means that the β-CDEDTA16 nanosponge is able to entrap much less water with respect to, for

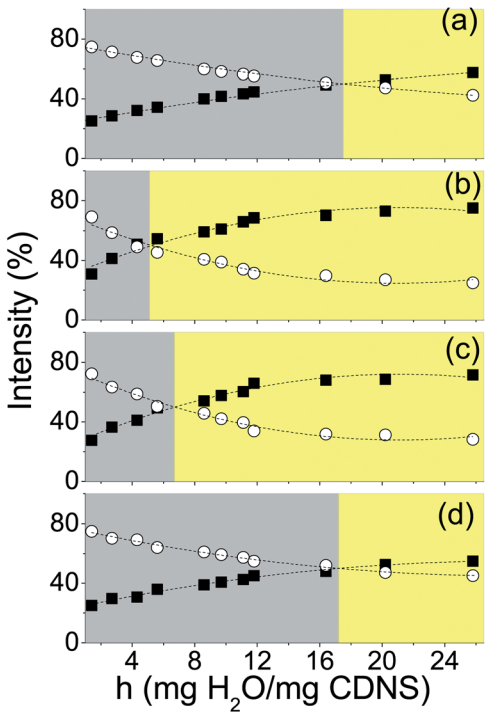

Fig. 5 Percentage intensities $I_1 + I_2$ (closed squares) and $I_3 + I_4$ (open circles) of the spectral contributions to the O–H stretching band, as a function of the hydration h, for (a) β-CDEDTA14, (b) β-CDEDTA16, (c) β-CDEDTA18, and (d) β-CDEDTA110 hydrogels. The vertical lines indicate the value estimated for h_{cross} (see text for details).

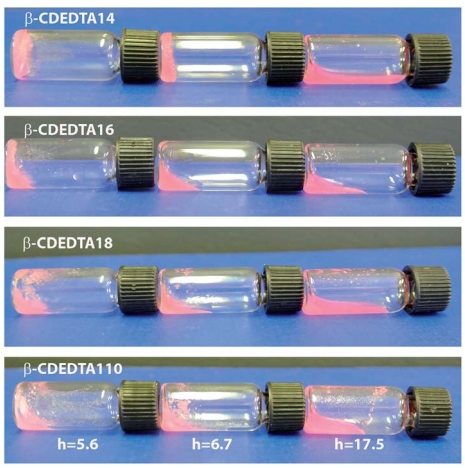

Fig. 6 Photographs of different phase behaviour for β-CDEDTA1*n* hydrogels as increasing the level of hydration h. Note: a suitable dye (Rhodamine B) was added to the water solvent in order to better visualize the phase changes of the system.

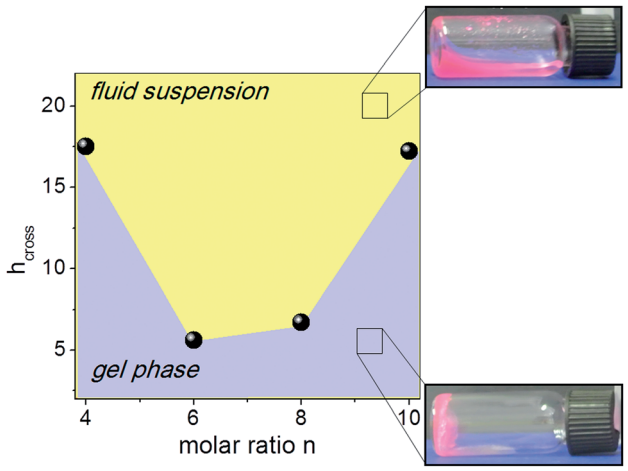

Fig. 7 Crossover hydration level h_{cross} estimated for nanosponge hydrogels as a function of the parameter n.

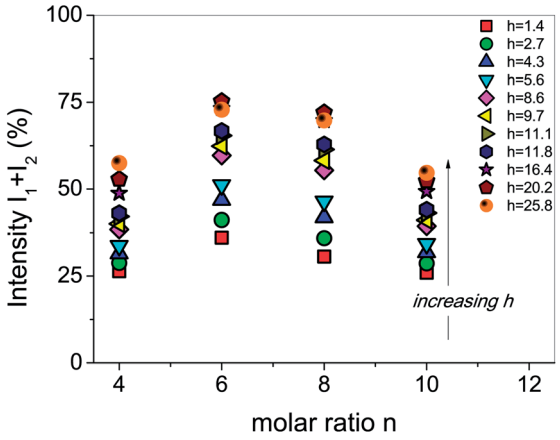

Fig. 8 Percentage intensities $I_1 + I_2$ reported as a function of the molar ratio n for different values of hydrations h, as indicated in the panel.

example, β-CDEDTA18 while β-CDEDTA14 and β-CDEDTA110 nanosponges appear to be the most absorbent polymers.

Two possible explanations to this occurrence can be given. On one side, the reduced ability of the β-CDEDTA16 nanosponge to adsorbing water can be ascribed to its highest rigidity, as proved by previous Brillouin and Raman measurements.[10,16] As a consequence, water molecules show reduced capability to enlarge the pores and a lower number of H_2O molecules are confined. Another reasonable hypothesis could be that the pores of the β-CDEDTA16 nanosponge may have smaller dimensions with respect to the other samples, as β-CDEDTA16 exhibits the highest cross-linking degree.

The interplay between the two factors reported above is currently being investigated by small angle neutron scattering and will be reported elsewhere.

Finally, a discussion of the behaviour, as a function of n, of the percentage intensities $I_1 + I_2$ at different hydration levels h is worth of mention.

In Fig. 8 an estimation of the quantity $I_1 + I_2$ is plotted, as a function of the parameter n, for each investigated hydration level h.

The maximum value of $I_1 + I_2$, *i.e.* the maximum value of the population corresponding to tetrahedral contributions, is always reached at $n = 6$. That is, whatever the hydration level is considered, at least in the explored h-range, the tetrahedral network of water molecules becomes prevalent in the β-CDEDTA16 nanosponge with respect to the others. This finding confirms that the properties observed for $n = 6$ in ester-based CDNS are deeply related to the structure of the polymeric network as obtained by the synthetic process.

Conclusions

Direct evidence of gel–sol phase transition in a new class of cyclodextrin-based hydrogel is given by monitoring the changes occurring in the vibrational dynamics of the system during its evolution.

The hydration of cyclodextrin nanosponges with progressively increasing amounts of water allowed us to follow the transition of the polymers from a state of a rigid gel into a liquid suspension. At the same time, measurements of the spectral changes occurring in the O–H stretching and HOH bending profile of water molecules progressively confined in the nano-pores of CDNS were carried out by using Fourier transform infrared spectroscopy in attenuated total reflectance geometry (FTIR-ATR). To this end, best-fitting and deconvolution procedures were employed for the separation of spectral components contributing to the O–H stretching band in order to account the connectivity pattern of water molecules concurring to the gelation process of CDNS.

The experimental data give evidence that the increase of the hydration level in nanosponges is accompanied by an enhancement of the population of H_2O molecules engaged in tetrahedral-coordinated hydrogen-bond networks. This configuration becomes dominant with respect to the no bulk-like contributions above a characteristic cross-over hydration level h_{cross}. As a main result, this crossover was demonstrated to be strictly correlated with the macroscopic properties of the system (*i.e.* the absorption ability of CDNS and rigidity of the corresponding hydrogel network) and to be strongly dependent, on the cross-linking agent/CD molar ratio.

These findings suggest the existence of a specific phase diagram of the cyclodextrin nanosponge hydrogels, where the parameter n plays a fundamental role in defining the nano- and microscopic properties of the system. Finally, these results provide a novel contribution to the rational comprehensive view of the chemical–physical interactions controlling the behaviour of self-assembled cyclodextrin-based systems over different length scales. Future efforts will be devoted to the study of the rheological properties of these hydrogels in order to better define their macroscopic mechanical properties.

Notes and references

1 W. Hamley, *Introduction to Soft Matter*, Wiley & Sons, 2007.
2 G. M. Whitesides and B. A. Grzybowski, *Science*, 2002, **295**, 2418.

3 K. Sakurada, F. M. McDonald and F. Shimada, *Angew. Chem., Int. Ed.*, 2008, **47**, 5718.
4 A. Atala, R. P. Lanza, J. A. Thomson and R. M. Nerem, *Principles of regenerative medicine*, Academic Press, Burlington, MA, 2008.
5 B. V. Slaughter, S. S. Khurshid, O. Z. Fisher, A. Khademhosseini and N. A. Peppas, *Adv. Mater.*, 2009, **21**, 3307.
6 F. Trotta and W. Tumiatti, Cross-linked polymers based on cyclodextrin for removing polluting agents, *WO Pat.*, 03/085002, 2003.
7 F. Trotta, W. Tumiatti, R. Cavalli, O. Zerbinati, C. M. Roggero and R. Vallero, Ultrasound-assisted synthesis of cyclodextrin-based nanosponges, *WO Pat.*,06/002814, 2006.
8 F. Trotta, V. Tumiatti, R. Cavalli, C. Rogero, B. Mognetti and G. Berta, Cyclodextrin-based nanosponges as a vehicle for antitumoral drugs, *WO Pat.*,09/003656 A1, 2009.
9 F. Castiglione, V. Crupi, D. Majolino, A. Mele, B. Rossi, F. Trotta and V. Venuti, *J. Phys. Chem. B*, 2012, **116**(43), 13133.
10 B. Rossi, S. Caponi, F. Castiglione, S. Corezzi, A. Fontana, M. Giarola, G. Mariotto, A. Mele, C. Petrillo, F. Trotta and G. Viliani, *J. Phys. Chem. B*, 2012, **116**(17), 5323.
11 F. Castiglione, V. Crupi, D. Majolino, A. Mele, W. Panzeri, B. Rossi, F. Trotta and V. Venuti, *J. Inclusion Phenom. Macrocyclic Chem.*, 2013, **75**(3–4), 247.
12 A. Mele, F. Castiglione, L. Malpezzi, F. Ganazzoli, G. Raffaini, F. Trotta, B. Rossi, A. Fontana and G. Giunchi, *J. Inclusion Phenom. Macrocyclic Chem.*, 2011, **69**, 403.
13 F. Castiglione, V. Crupi, D. Majolino, A. Mele, B. Rossi, F. Trotta and V. Venuti, *J. Phys. Chem. B*, 2012, **116**(27), 7952.
14 F. Castiglione, V. Crupi, D. Majolino, A. Mele, B. Rossi, F. Trotta and V. Venuti, *J. Raman Spectrosc.*, 2013, **44**(10), 1463.
15 V. Crupi, D. Majolino, A. Mele, B. Rossi, F. Trotta and V. Venuti, *Soft Matter*, 2013, **9**, 6457.
16 V. Crupi, A. Fontana, M. Giarola, D. Majolino, G. Mariotto, A. Mele, L. Melone, C. Punta, B. Rossi, F. Trotta and V. Venuti, *J. Raman Spectrosc.*, 2013, **44**(10), 1457.
17 L. Seglie, K. Martina, M. Devecchi, C. Roggero, F. Trotta and V. Scariot, *Postharvest Biol. Technol.*, 2011, **59**, 200.
18 B. B. Mamba, R. W. Krause, T. J. Malefetse, G. Gericke and S. P. Sithole, *Water*, 2008, **34**, 657.
19 M. Arkas, R. Allabashi, D. Tsiourvas, E. M. Mattausch and R. Perfler, *Environ. Sci. Technol.*, 2006, **40**, 2771.
20 L. Liang, L. De-Pei and L. Chih-Chuan, *Eur. J. Biochem.*, 2002, **269**, 5753.
21 F. Trotta, M. Zanetti and R. Cavalli, *Beilstein J. Org. Chem.*, 2012, **8**, 2091.
22 P. K. Shende, F. Trotta, R. S. Gaud, K. Deshmukh, R. Cavalli and M. Biasizzo, *J. Inclusion Phenom. Macrocyclic Chem.*, 2012, **74**, 447.
23 F. Trotta, R. Cavalli, K. Martina, M. Biasizzo, J. Vitillo, S. Bordiga, P. Vavia and J. Ansari, *J. Inclusion Phenom. Macrocyclic Chem.*, 2011, **71**, 189.
24 S. Swaminathan, L. Pastero, L. Serpe, F. Trotta, P. R. Vavia, D. Aquilano, M. Trotta, G. Zara and R. Cavalli, *Eur. J. Pharm. Biopharm.*, 2010, **74**, 193.
25 D. Lembo, S. Swaminathan, M. Donalisio, A. Civra, L. Pastero, D. Aquilano, P. Vaviac, F. Trotta and R. Cavalli, *Int. J. Pharm.*, 2013, **443**, 262.
26 E. Memisoglu-Bilensoy, I. Vural, A. Bochot, J. M. Renoir, D. Duchene and A. A. Hincal, *J. Controlled Release*, 2005, **104**, 489.
27 R. Cavalli, A. Akhter, A. Bisazza, P. Giustetto, F. Trotta and P. Vavia, *Int. J. Pharm.*, 2010, **402**, 254.
28 F. Van de Manakker, T. Vermonden, C. F. Van Nostrum and W. E. Hennink, *Biomacromolecules*, 2009, **10**, 3157.
29 J. Li, *NPG Asia Mater.*, 2010, **2**, 112.
30 W. Liang, C. Yang, D. Zhou, H. Haneoka, M. Nishijima, G. Fukuhara, T. Mori, F. Castiglione, A. Mele, F. Caldera, F. Trotta and Y. Inoue, *Chem. Commun.*, 2013, **49**, 3510.
31 M. Rubinstein and R. H. Colby, *Polymer Physics*, Oxford University Press Inc., New York, 2003.
32 E. Zaccarelli, *J. Phys.: Condens. Matter*, 2007, **19**, 323101.
33 V. Crupi, F. Longo, D. Majolino and V. Venuti, *J. Phys.: Condens. Matter*, 2006, **18**, 3563.
34 R. Langer and D. A. Tirrell, *Nature*, 2004, **428**, 487.
35 A. M. Kloxin, A. K. Kasko, C. N. Salinas and K. S. Anseth, *Science*, 2009, **324**, 59.
36 J. D. Eaves, J. J. Loparo, J. C. Fecko, S. T. Roberts, A. Tokmakoff and P. L. Geissler, *Proc. Natl. Acad. Sci. U. S. A.*, 2005, **102**, 13019.
37 D. P. Schofield, J. R. Lane and H. G. Kjaergaard, *J. Phys. Chem. A*, 2007, **111**, 567.
38 N. Goldman and R. J. Saykally, *J. Chem. Phys.*, 2004, **120**, 4777.
39 F. Mallamace, M. Broccio, C. Corsaro, A. Faraone, D. Majolino, V. Venuti, L. Liu, C. Y. Mou and S. H. Chen, *Proc. Natl. Acad. Sci. U. S. A.*, 2007, **104**, 424.
40 J. B. Brubach, A. Mermet, A. Filabozzi, A. Gerschel, D. Lairez and M. P. Krafft, *J. Phys. Chem. B*, 2001, **105**, 430.
41 R. Stancanelli, R. Ficarra, C. Cannavà, M. Guardo, M. L. Calabrò, P. Ficarra, R. Ottanà, R. Maccari, V. Crupi, D. Majolino and V. Venuti, *J. Pharm. Biomed. Anal.*, 2008, **47**, 704.
42 I. Bratu, F. Veiga, C. Fernandes, A. Hernanz and J. M. Gavira, *Spectroscopy*, 2004, **18**, 459.
43 V. Crupi, S. Interdonato, F. Longo, D. Majolino, P. Migliardo and V. Venuti, *J. Raman Spectrosc.*, 2008, **39**, 244.
44 P. A. Giguère, *J. Chem. Phys.*, 1987, **87**, 4835.
45 K. B. Møller, R. Rey and J. T. Hynes, *J. Phys. Chem. A*, 2004, **108**, 1275.
46 C. P. Lawrence and J. L. Skinner, *Chem. Phys. Lett.*, 2003, **369**, 472.
47 V. Crupi, F. Longo, D. Majolino and V. Venuti, *Eur. Phys. J.: Spec. Top.*, 2007, **141**, 61.